Evaluation of Shear Modulus and Damping in Dynamic Centrifuge Tests

A.J. Brennan[1], N.I. Thusyanthan[2] &
S.P.G. Madabhushi[3]

CUED/D-SOILS/TR336 (2004)

[1] Research Fellow, Wolfson College, University of Cambridge

[2] Research Student, Girton College, University of Cambridge

[3] Senior Lecturer, Girton College, University of Cambridge

Evaluation of Shear Modulus and Damping in Dynamic Centrifuge Tests[4]

Cambridge University Engineering Department

Technical Report
CUED/D-SOILS/TR336

A.J. Brennan, N.I. Thusyanthan & S.P.G. Madabhushi

October 2004

Summary

Correct evaluation of shear modulus and damping characteristics in soils under dynamic loading is key to both the fundamental understanding of soil behaviour and the practical application of soil modelling programs. Dynamic centrifuge tests can contribute significant information about soil behaviour, but great care must be taken over the signal processing techniques involved, and the test conditions are different from the laboratory experiments that form the database of existing knowledge. This paper outlines several factors that require careful consideration when deriving stiffness and damping parameters from centrifuge data. Shear modulus and damping degradation curves for a dry sand, saturated sand, soft clay and a model waste are then evaluated to explore some of the factors that are introduced during centrifuge tests. Stiffness is seen to be a more reliable parameter than damping ratio. Damping during centrifuge tests for certain materials appeared to differ from the expected values.

[4] An extension of the paper submitted to the ASCE Journal of Geotechnical and Geoenvironmental Engineering in September 2004.

1 Introduction

The cyclic shear stress-shear strain behaviour of soils is key to an understanding of how sites will respond to applied shear loads such as those created by an earthquake. This is nonlinear and hysteretic. Numerical soil models use the variation of shear modulus and damping with strain level, G-γ and D-γ curves, as fundamental input parameters for dynamic analyses. These would ordinarily be based on element tests carried out, either on the specific material in question or on representative similar materials published in the literature.

Dynamic centrifuge testing represents an alternative technique for investigating soil behaviour. As real soil is used, there is no dependence on model parameter values, and stresses and strains are transferred without the confines of an element test. However, data may only be obtained as a time series of values recorded by available instrumentation at specific points. Instrumentation and data acquisition quality provide the constraints. This paper will present a simple technique for using centrifuge accelerometer data to determine both shear modulus and damping in soils undergoing base shaking at multiple input frequencies. Back-calculation of damping in particular is a largely unexplored area. Several important considerations in handling data are discussed. A selection of centrifuge data from a variety of soils will then be used to compare values obtained with those in previously published data/design curves, to investigate the effects of centrifuging on modulus and damping. The scaling associated with centrifuge testing at N times earth's gravity recreates prototype stress and strain, but other factors are also changed. In particular the frequency of dynamic events is N times faster, which could have an effect on the soil response.

2 Shear Moduli and Damping in Soils

The relative importance of parameters affecting shear modulus and damping were summarised by Hardin & Drnevich (1972a). Shear strain amplitude, effective stress level and void ratio were listed as affecting shear modulus most in clean sands. Damping was considered to be affected by these too, with number of loading cycles also being a major factor. For clays, the number of loading cycles has been correlated to a decrease in shear modulus with associated pore pressure increase, as summarised by Idriss et al (1978). Overconsolidation ratio and plasticity index are also influential in clay behaviour.

Many studies have used cyclic triaxial or resonant column tests to determine these parameters as functions of shear strain and effective stress for various materials, for example, gravels (Seed et al, 1986, Rollins et al, 1998), sands (Wilson, 1988, Kokusho, 1980), loess (Hardcastle & Sharma, 1998) and clays (Idriss et al, 1978, Kokusho et al, 1982, Vucetic & Dobry, 1991). Field studies have also been carried out to investigate stiffness nonlinearity, based on earthquake motions (Chang et al, 1989, Zeghal & Elgamel, 1994, Zeghal et al, 1995). Such fieldwork can unfortunately only occur on the few instrumented sites. Centrifuge testing avoids the limitations in soil type available in a field test, and the physical constraints of an element test.

It is not common to see centrifuge data used to develop stress-strain loops, or derive stiffness and damping parameters. Ellis et al (1998) derive modulus and damping of very dense sand saturated with different pore fluids based on centrifuge work carried out in Japan. Teymur & Madabhushi (2002) generated stress-strain loops to exemplify wavelet techniques and describe boundary effects in centrifuge packages. Pitilakis et al (2004) plotted some first order loops to compare centrifuge and numerical data. Arulnathan et al (2000) and Ghosh & Madabhushi (2002) back-calculated G_{max} from measured shear wave velocities using air-hammer devices. With centrifuge testing, there is an added complication of scaling laws. The important issues to bear in mind here are the use of viscous pore fluids to match seepage and dynamic time scales, and the increased loading frequencies that must be used to represent lower prototype frequencies.

3 Data Handling

Data described here is obtained from centrifuge tests, where accelerometers are typically arranged in columns containing between 3 and 6 instruments. Accelerations ü are obtained from which parameters must be inferred. The instruments used in this work are D.J. Birchall type A/23 charge-based accelerometers. Response characteristics of accelerometers obviously vary between make and model, but these particular instruments have a poor response at low frequencies (-3 dB at 4 Hz) which has implications when performing numerical integration. Demonstrative examples shown in this section are from three accelerometers aligned vertically in a dense/medium dense level bed of dry Hostun S28 sand (as section 4.1), described further by Pitilakis et al (2004).

Recorded accelerations by instrument number *i* at depth z_i are written as $\ddot{u}_i$ (= $\ddot{u}(z_i)$).

3.1 Calculation of Shear Stress

From the original shear beam equation, shear stress τ at any depth z may be written as the integration of density ρ times acceleration $\ddot{u}$ through higher levels (Equation 1).

$$\tau(z) = \int_0^z \rho \ddot{u} dz \tag{1}$$

The equations proposed by Zeghal & Elgamel (1994) for field measurements utilise acceleration measured at the surface as they deal with site data. In contrast, a reliable surface acceleration is rarely available in centrifuge testing as the instrument needs to be buried to maintain good contact with the soil. A linear fit is therefore recommended between adjacent pairs of instruments, which may be extrapolated from the top pair to the surface (Equation 2). If many accelerometers are present, and significant amplification/attenuation is observed, a trapezoidal integration can be used to obtain shear stress. In many centrifuge tests, neither apply. Therefore shear stress is evaluated using Zeghal & Elgamel's expression (Equation 3) with the interpolated surface acceleration obtained from Equation 2 with z = 0.

$$\ddot{u}(z) = \ddot{u}_1 + \frac{(\ddot{u}_2 - \ddot{u}_1)}{(z_2 - z_1)}(z - z_1) \tag{2}$$

$$\tau(z) = \frac{1}{2}\rho z(\ddot{u}(0) + \ddot{u}(z)) \tag{3}$$

Direct integration of the linear approximation for $\ddot{u}$ (Equation 2) may also be applied to obtain the same result. Equation 4 demonstrates this for shear stress at depth z_2.

$$\tau(z_2) = \frac{1}{2}\rho \frac{(\ddot{u}_1 z_2^2 + \ddot{u}_2 z_2 (z_2 - 2z_1))}{(z_2 - z_1)} \tag{4}$$

3.2 Calculation of Shear Strain

Two methods of shear strain calculation are available, a first or a second order expression. Displacement must first be obtained from the acceleration recordings. Recorded data used for this work contained about 0.15s of data prior to the start of shaking, and a certain amount of time after shaking has stopped, in which noise and ambient vibration is present. It is possible to cut these parts from the signal prior to processing. However the effects of filtering (see below) can introduce unwanted errors if

the extreme ends of the data signal are non-zero, as the filter is effectively being applied to a step function. Therefore it is safer to leave these extraneous datapoints present, and to force them to equal zero while there is no shaking. This will prevent the noise being integrated to produce finite displacements before loading, and also prevent the filter-induced perturbations interfering with the signal.

Acceleration data must be band-filtered prior to integration (see below) to produce velocity, and then filtered again before being integrated to displacement u. This is important as low frequency information present in the velocity trace is common and produces a characteristic linearly varying displacement that continues changing after the end of shaking. Examples of this exist in published literature.

If only two instruments are present in a given soil layer, as would be common when testing soil conditions that change with depth or instrument malfunction is experienced, a simple first order approximation must be applied (Equation 5). This applies for any point between instruments 1 and 2, and as such is more appropriate for the mid-point.

$$\gamma = \frac{(u_2 - u_1)}{(z_2 - z_1)} \tag{5}$$

If three instruments are stacked in a soil column then a better, second order approximation may be made (Equation 6). This would apply at depth z_i. Equation (6) is also part of the Zeghal & Elgamel work.

$$\gamma(z_i) = \left[(u_{i+1} - u_i)\frac{(z_i - z_{i-1})}{(z_{i+1} - z_i)} + (u_i - u_{i-1})\frac{(z_{i+1} - z_i)}{(z_i - z_{i-1})} \right] \Big/ (z_{i+1} - z_{i-1}) \tag{6}$$

Figure 1 shows the differences between these two methods for a typical test. The second order expression seems to be able to "iron out" small discrepancies that produce some large peaks in the first order expression. The figure is included as a guide to the strains calculated by the two expressions.

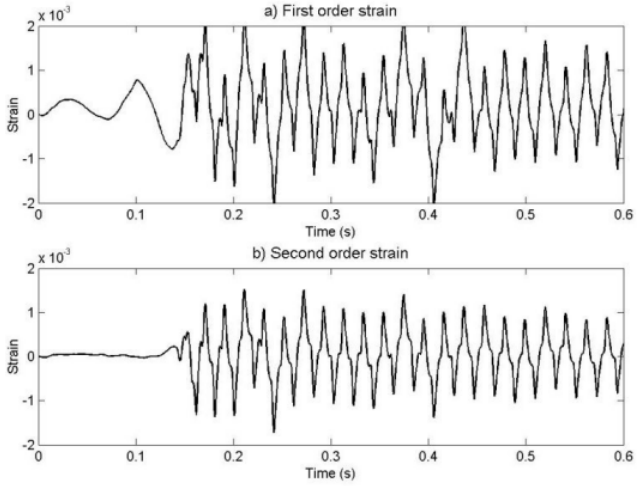

Figure 1. Strains calculated based on a) first order and b) second order approximations.

3.3 Calculation of Shear Modulus

Having obtained shear stress and shear strain, a plot of one against the other enables evaluation of shear modulus. A reliable method must be found for finding representative slopes through loops such as the one illustrated in Figure 2, where higher frequency loading components affect the curve and produce many tangent changes. The most reliable method of producing representative moduli has been to evaluate the difference in maximum and minimum stress applied during a loop, and the difference in maximum and minimum strain developed in that loop. The ratio of these two values has been used throughout for shear modulus calculation, and is plotted as a dashed line on Figure 2.

To compare measured shear moduli with standard degradation curves also requires a value for the small-strain shear modulus G_{max} against which shear modulus is usually normalised. Test data shown in section 4 is normalised by a G_{max} obtained from equation (7), where V_s is shear wave velocity and ρ soil density. For the model waste and the saturated sand, shear wave velocity V_s is obtained using a miniature air hammer which operates at strains around 0.03% (Ghosh & Madabhushi, 2002). For the dry sand and the clay no such data is available. V_s for the clay is estimated by dividing time lag between pairs of accelerometers (from cross-correlation of earthquake signals) by separation distance. It would be expected that the value of G_{max} obtained this way would be less than the actual value due to the increased strains. In the dry sand, waves travelled too quickly to allow an accurate estimate of time lag to be made. The natural frequency of the

soil layer f_0 was obtained from the calculated transfer function, and shear wave velocity estimated using Eq. (8), in which H is soil layer thickness.

$$G_{\max} = V_s^2 \rho \tag{7}$$

$$V_s = 4Hf_0 \tag{8}$$

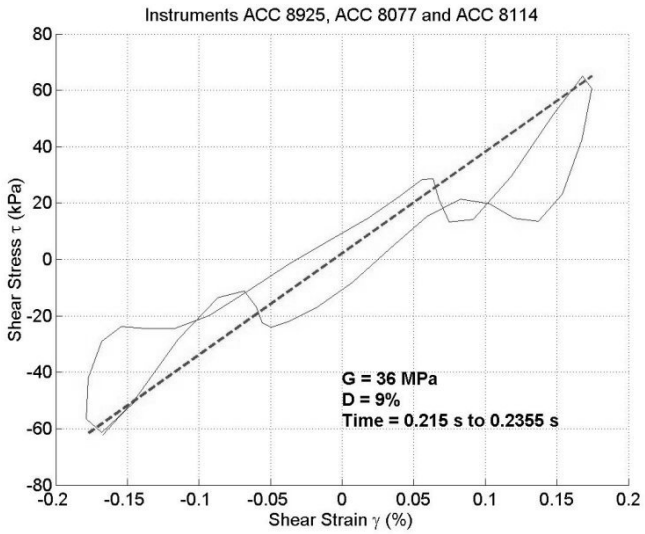

Figure 2. Stress strain loop for a particular multi-frequency loading of dry sand.

3.4 Calculation of Equivalent Damping Ratio

It is rare to find estimation of damping values from acceleration records in the literature. Data such as that from Abdel-Ghaffar & Scott (1979) has been based on heavily filtered data that leaves nice clean ellipses whose area may readily be calculated. Data from laboratory tests has been based on true single frequency loading so areas may also be calculated easily. For evaluation of damping during centrifuge experiments it must be remembered that actual loading frequencies are many times the frequency being interpreted (here, 50+ times greater), and also many times larger than frequencies commonly used in element testing.

Back-calculation of damping is performed at the stress-strain loop stage. A simple trapezoidal integration between datapoints is used to estimate the area inside the bounds of the loop representing work done W. Figure 2 shows a potential source of error. High frequency components of loading, which are real stresses and not noise, cause the curves to cross, as seen for the small regions at about 0.08% and – 0.08% shear strain in Figure 2. The net effect of these upon integration is negative; work *appears* to be released by the system rather than absorbed. The contribution of such crossover areas have been taken

as a guide to the accuracy of any given damping estimate in a loop. A net negative damping for a complete loop, as might be produced if one of the instruments has malfunctioned, is not possible as this contravenes the second law of thermodynamics.

The equivalent damping ratio is defined in the conventional way, Equation (9), by dividing net work done by 2π times the work that would be retrieved if the system was elastic with stiffness G. It is evaluated by taking ¼ times the total stress range Δτ times the total strain range Δγ.

$$D = \frac{1}{2\pi}\frac{W}{W_{elastic}} = \frac{1}{2\pi}\frac{\oint \tau d\gamma}{\left(0.25 \times \Delta\tau \times \Delta\gamma\right)} \tag{9}$$

Thus damping is calculated using the area of the actual stress-strain loop.

3.5 Appropriate Data Filtering

It is important to filter data at high frequency to eliminate noise and at low frequency to eliminate drift errors during integration. Unlike many laboratory experiments, the loading applied by a centrifuge earthquake actuator is not necessarily single frequency. Higher harmonics of the main shaking frequency can exist, that are real loading components and not noise. Therefore their presence affects the response and they should not be filtered out. Also, earthquake actuators are increasingly being made to apply multi-frequency loading, such as those at UC Davis and RPI in the US, and HKUST in Hong Kong.

The purpose of this section is to illustrate the effects of inappropriate filtering, quantified with a specific example. Variations in equipment between institutions will naturally affect error magnitude and choice of filtering frequency.

Figure 3 shows an input acceleration and Fourier spectra for the signal (unfiltered) used to create the loops in Figure 2, Figure 4 and Figure 5. It can be seen that in addition to the main driving frequency of 50 Hz, significant harmonics are present at 150 Hz, 250 Hz and even 350 Hz. Filtering was performed at 20 Hz – 450 Hz to produce Figure 2. The effect of not filtering at all on the stress-strain loop is shown in Figure 4.

By not filtering it is seen that the strain axis in particular is completely wrong as low-frequency drift has caused the signal to walk away from the zero strain origin. The

calculated shear modulus is too low as the strain range appears larger than it should due to superimposed drift. Calculated damping is nonsensical as the loop does not close.

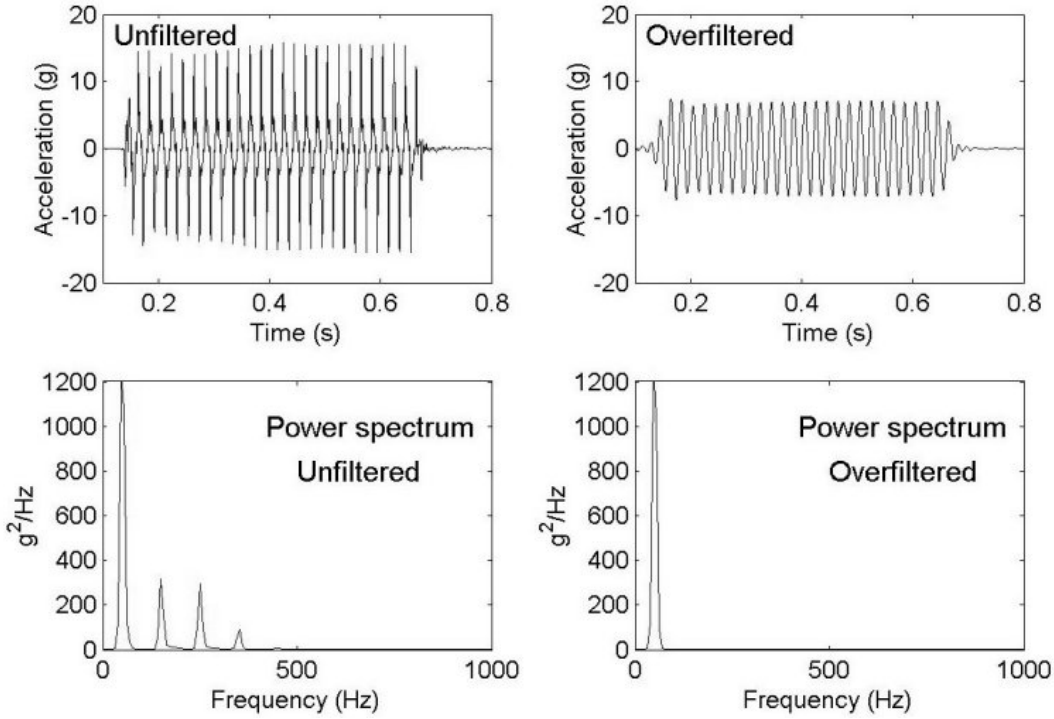

Figure 3. Frequencies present in a typical motion, and the effects of overfiltering data.

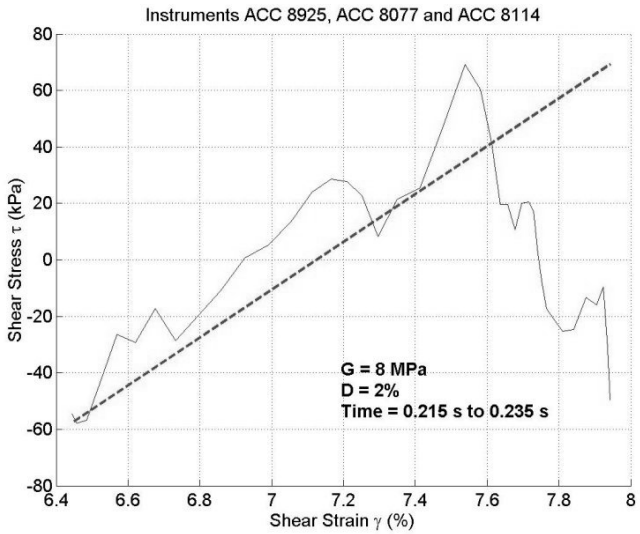

Figure 4. "Walking" errors associated with unfiltered low-frequency accelerometer drift.

This much is well understood, but more common are loops such as Figure 5, which has been produced by applying a bandpass filter between 20 Hz and 70 Hz to the same data shown in Figure 2. Only the first harmonic of shaking frequency remains. By filtering out

the higher harmonics the loop appears closer to those published as a result of laboratory tests, where single frequency vibration has really been applied, and create a very nice picture. No "walking" errors are experienced as the low frequencies have been eliminated. However, elimination of higher frequency components removes the detail of the actual load path, and increases the calculated damping. The loop in Figure 5 is fatter than that in Figure 2; 8% damping appeared to increase to 13%. Also removed is the detail of the sharpness at the stress peak. Peak stress in Figure 5 is reduced from the 65 kPa (Figure 2 and Figure 4) to about 39 kPa and the crest is rounded off, and therefore a corresponding decrease in recorded shear modulus is experienced (36 MPa reduced to 25 MPa). Figure 3 shows the time trace of this signal and its Fourier spectrum, which is clearly somewhat distorted from the loads that have really been applied.

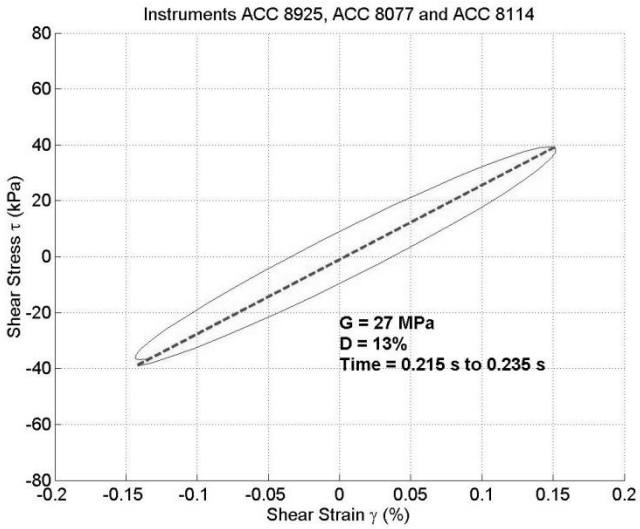

Figure 5. Incorrect, overfiltered stress-strain loop for the data in Figure 2 and Figure 3.

High frequency data may also be present in the soil response. Figure 6 shows the method as applied to saturated sand. The stress-strain response is shown for several loading cycles, after the first two cycles have already passed, generating significant excess pore pressures. Stiffness is considerably reduced except when large strain is applied in which case the soil begins to dilate and a sudden stiffening is seen. After the large stress cycle, however, the soil has become too soft and is not transmitting shear waves significantly any more. This dilation effect creates high frequencies in the soil that are not present in the applied loads. The secant shear modulus calculated now appears to be a nonsensical value (of 0.75 MPa) whereas in fact two distinct stiffnesses are seen during the loading cycle.

Actual filtering frequencies used are of course totally dependant on the spectrum of input motion, as is the magnitude of error derived from excessive filtering.

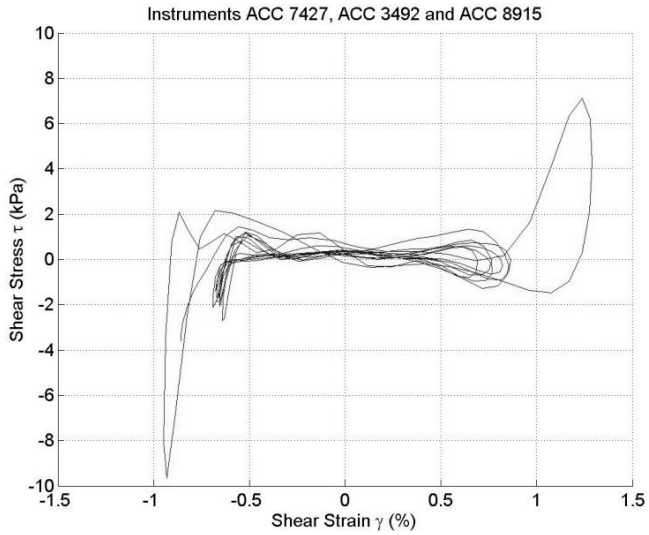

Figure 6. High frequency components generated by soil response; here through dilation.

4 Shear Modulus from Centrifuge Tests

In this section, the method described will be applied to evaluate shear modulus degradation curves from centrifuge tests on four different geotechnical materials, summarised in Table 1.

Table 1. Properties of materials investigated.

	Dry sand	**Saturated sand**	**Clay**	**Model waste**
Specification	Hostun S28	Fraction E	E-grade kaolin	Peat/clay/sand
Pore fluid	none	50 cSt silicone oil	water	water
Density (kg/m^3)	1600	1900	1660	1000
Voids ratio e	0.68	0.80	1.45	2.26
Moisture content	0%	30%	55%	23%
D_{50} (μm)	150	140	5	380
V_s (m/s)	200	145-170	70	70
Permeability k (m/s)	N/A	10^{-4}	5×10^{-8}	N/A
Plasticity Index	0	0	21	0

All tests described have been carried out at 50-g on the Cambridge 10-m diameter beam centrifuge (Schofield, 1980). Earthquake motion is applied using the mechanical stored

angular momentum actuator described by Madabhushi et al (1998), for which a typical input motion would be as in Figure 3. Between 15 and 25 cycles are usually applied, at target frequencies from 30-50 Hz (modelling prototype earthquakes between 0.6 and 1 Hz). Harmonics of input frequency are generated by the mechanical system (as in Figure 3) and other higher frequency data may be generated by soil response (as in Figure 6).

4.1 Dry Sand

Hostun S28 sand was used in a series of dry tests for the EU-funded NEMISREF project (Pitilakis et al, 2004). This sand is uniformly graded with D_{50} = 0.15 mm, e_{min} = 0.62 and e_{max} = 1.01. Sand was poured dry to a mean voids ratio of e = 0.68 and a depth of 340 mm. Shear moduli are derived from 4 accelerometers aligned vertically up the centre of the benchmark model. Figure 7 shows these for the deeper 3 (σ_{vo}' = 192 kPa at the middle instrument) and Figure 8 shows the shallower 3 (σ_{vo}' = 112 kPa). These are normalised by a G_{max} value of 64 MPa, derived from a shear wave velocity inferred from the soil's natural frequency. Using the expression by Hardin & Drnevich (1972b) gives 119 MPa and 91 MPa instead.

Also plotted on the graphs are curves generated from the equations given by Hardin & Drnevich (1972b) for dry fine sands, and by Rollins et al (1998) for gravels, whose best fit curve is also shown to fit data for sands. A best fit through appropriate resonant column data presented by LoPresti et al (1998) is also plotted.

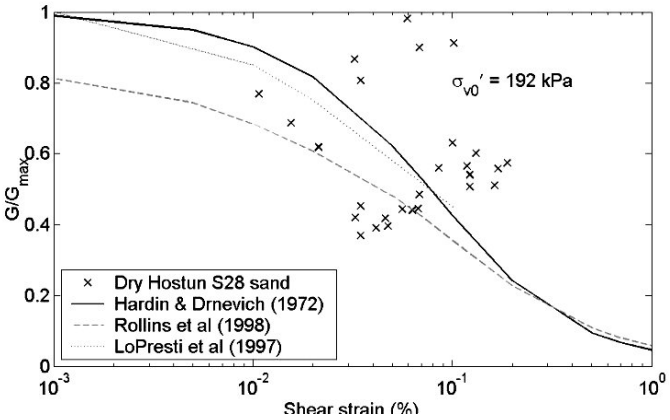

Figure 7. Shear modulus degradation of dry sand, σ_{v0}' = 192 kPa.

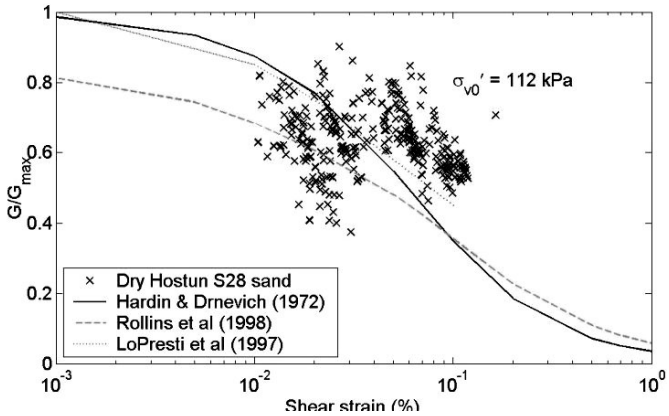

Figure 8. Shear modulus degradation of dry sand, σ_{v0}' = 112 kPa.

Both Figure 7 and Figure 8 show centrifuge data is a reasonable match to the standard curves/element test data, and is apparently better at smaller (< 0.05%) strains. There is, however, a large degree of scatter, particularly at the higher stress (Figure 7). This does not correlate with cycle number and must be put down to inherent variability in available measurements.

4.2 Saturated Sand

Fraction E silica sand saturated with silicone oil at 50 cS viscosity was used for a series of centrifuge tests in the PhD work of Brennan (2004). This sand is uniformly graded with D_{50} = 0.14 mm, e_{min} = 0.61 and e_{max} = 1.01. Sand was poured dry to a mean voids ratio of around e = 0.8, then saturated under vacuum with silicone oil at 50 cS viscosity.

Excess pore pressure build up and the associated acceleration reduction makes shear modulus a harder parameter to obtain from liquefiable sands. Only the first cycle of loading is considered for the data presented, where a clear shear stiffness could be obtained. Stress-strain curves such as that in Figure 6 are not demonstrating the sort of behaviour that can be classified by a stiffness. Figure 9 shows the data from deeper models, and Figure 10 data obtained from less deep models. Shear moduli are normalised with respect to G_{max} calculated from shear wave velocity measured in the same sand by Ghosh & Madabhushi (2002). Comparison curves are from Hardin & Drnevich (1972b) and Ishibashi & Zhang (1993).

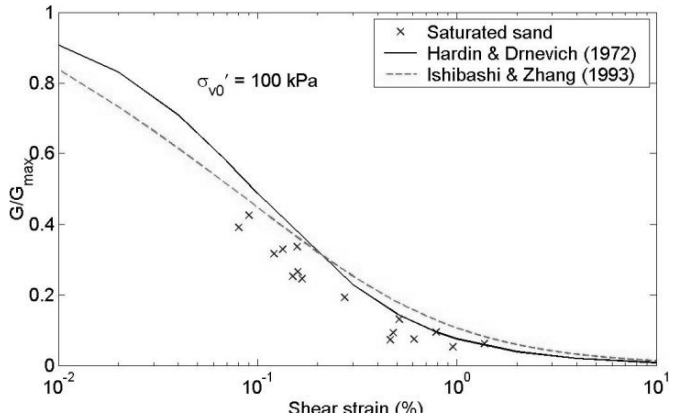

Figure 9. Shear modulus degradation of saturated sand, σ_{v0}' = 100 kPa.

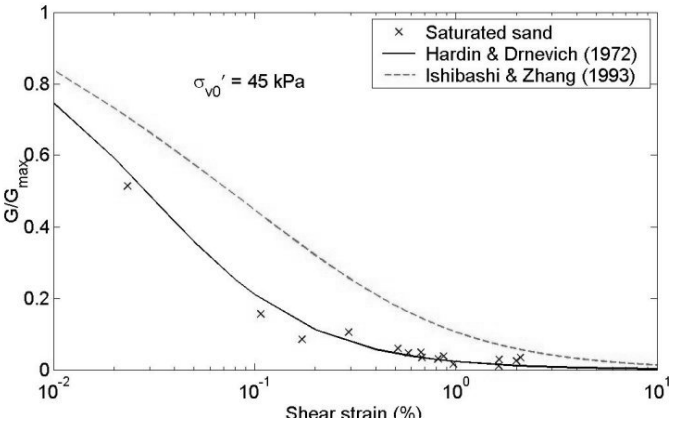

Figure 10. Shear modulus degradation of saturated sand, σ_{v0}' = 45 kPa

The centrifuge data is remarkably close to the Hardin & Drnevich curve in both cases. The Ishibashi & Zhang curve is a better fit at the higher effective stress. Interestingly, normalising data using G_{max} derived from the Hardin & Drnevich equation (66 MPa and 44 MPa) instead of from measured shear wave velocity produces (56 MPa and 40 MPa) a poorer fit. Data in that case lies below the line. That would imply that the shear wave velocity obtained from the air hammer is a reasonable value, and that the Hardin & Drnevich expression for G_{max} is a little too stiff for this case.

4.3 Normally Consolidated Clay

E-grade kaolin clay was used in a test carried out by Brennan et al (2002). The clay is normally consolidated and the pore fluid is water. 3 accelerometers are used, with an initial vertical effective stress of 62 kPa at the middle one. Data has been taken from different times during the 15-25 loading cycles of each earthquake to obtain a range of

strains. According to experience (e.g. Idriss et al, 1978) shear modulus reduces with number of cycles, possibly if excess pore pressures build up. However, no significant pore pressure generation was observed during these experiments, and no correlation was here observed between measured G values and number of cycles. Normalising parameter G_{max} has been derived from time lags between accelerometers during earthquakes.

Data is plotted in Figure 11 against the design curves of Hardin & Drnevich (1972b), Vucetic & Dobry (1991) and Ishibashi & Zhang (1993). Also included is a best fit curve through appropriate data from cyclic simple shear and resonant column tests on marine clays reported by Kagawa (1992).

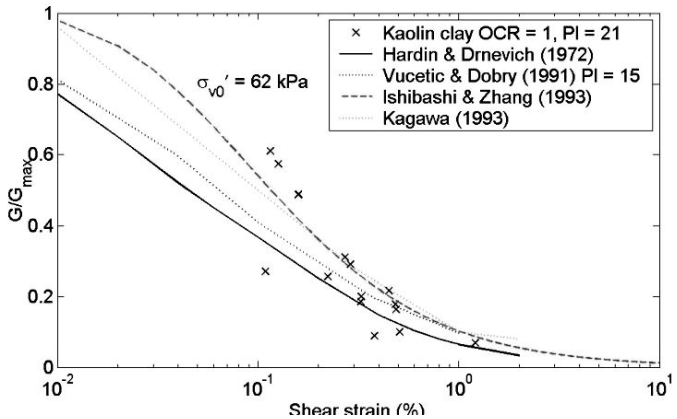

Figure 11. Shear modulus degradation of normally consolidated clay, PI = 21, σ_{v0}' = 62 kPa

The centrifuge data in Figure 11 displays the trend and values that would be expected throughout the strain range tested. However, the three points above the line at around 0.1% strain indicate that perhaps the small-strain response is stiffer than would be expected. This may be due to the approximation for G_{max}, 7.5 MPa. The Hardin & Drnevich expression yields 24 MPa which, as with the sands, would have been too stiff.

4.4 Model Municipal Solid Waste

An artificial municipal solid waste was produced by Thusyanthan et al (2004a) for investigating the dynamic behaviour of landfill systems. A mixture of sand, clay and peat in the mass ratio 1:1:1 was selected, which has static soil parameters representative of real municipal solid waste but none of the associated variability and handling problems. To determine how suitable the dynamic properties of this model material were, the method

is applied to recorded accelerometer data as before, and normalized derived shear modulus values are plotted in Figure 12.

Also plotted are the bounds derived by Augello et al (1998) by back analysing 5 past earthquakes on landfill material, and the bounds derived by Matasovic & Kavazanjian (1998) based on cyclic simple shear tests with back analysis of strong motion data. Matasovic & Kavazanjian had a wide amount of scatter in their test data in the 0.1-10% strain range, but recommend the upper bound for use in practice.

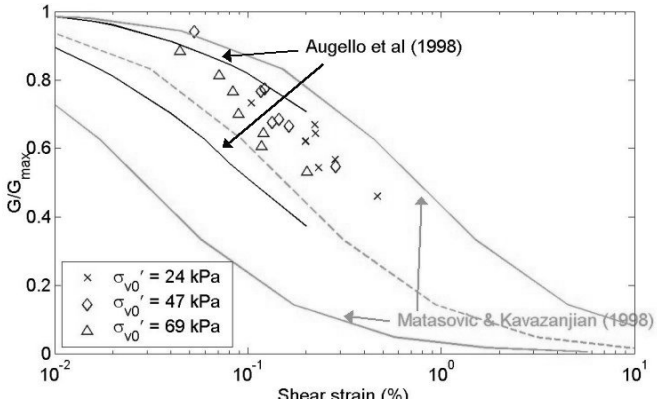

Figure 12. Shear modulus degradation of a model MSW mix.

The variable nature of landfill material means that the margins for MSW are a lot wider, However the centrifuge data provides a remarkably good fit, even within the tighter bounds of Augello et al, and closer to the recommended (upper bound) line from Matasovic & Kavazanjian. This close fit strongly supports the use of the model mixture for dynamic modelling of landfill systems (Thusyanthan et al., 2004b).

5 Equivalent Damping Ratio from Centrifuge Tests

In this section, the method is used to estimate damping values as functions of shear strain during centrifuge model earthquakes. Providing a single suitable loop is chosen containing sufficient datapoints, then a simple numerical integration around the cycle should provide the numerator of equation (9). As described in section 3.4, the loop from which damping is calculated must be representative of hysteretic damping, or the numerical integration will return an inaccurate value, particularly if the stress-strain curve crosses itself in such a way as to subtract from the net result.

Damping has been acknowledged (Hardin & Drnevich, 1972a, Teachavorasinskun et al, 2001) to be more affected by loading frequency than shear modulus is. This becomes an issue in centrifuge modelling where loading frequencies are necessarily increased to account for the accelerated time scale. Typical loading from an earthquake that would occur at the order of 1Hz is carried out at 30-100Hz on the centrifuge, and the shaking device may introduce additional higher frequency loads, so it is important to know which materials will experience this, and to what degree.

5.1 Dry Sand

The loops from the tests described in section 4.1 are used to generate the damping ratios plotted in Figure 13. Seed et al (1986) report that the influence of effective stress is only significant in laboratory tests for very low stresses (< 25 kPa), so data from both stress levels is plotted on the same axes. Rollins et al (1998) support this by measuring only a slight reduction in damping (about 2%, strain independent) as stress increases from 50 – 400 kPa. Also in Figure 13 are curves from the equations of Hardin & Drnevich (1972b) and Rollins et al (1998).

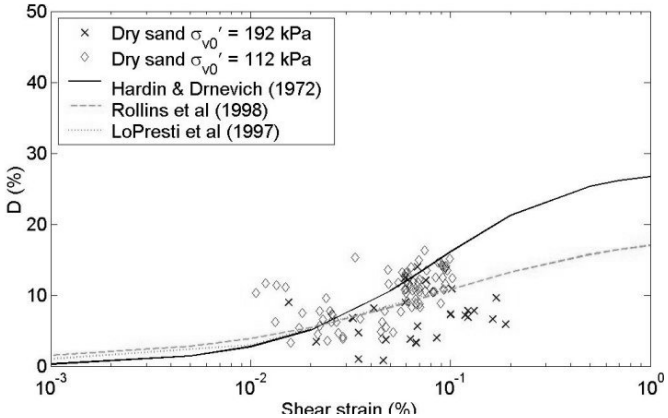

Figure 13. D-γ relationships for dry sand.

Data at the higher stress level seems to be on or just below the curve. This sort of scatter is commonly seen in investigations of damping, such as those used to derive the comparative information. At the lower stress level, centrifuge data fits well with the curves; they seem to form reasonable bounds for the data.

Analyses show that the point in the time record (i.e. number of cycles) where the data was obtained does not correlate with damping ratio, so this perhaps indicates that mean

confining pressure has more influence on the hysteretic damping of this sand than on those tested in the other studies.

5.2 Saturated Sand

Data for saturated sand (test described in table 1) is plotted in Figure 14 for the higher stress level and Figure 15 for the lower stress level. This data is more limited as the calculated damping is not always representative, as described in section 3.4. As with the modulus data, only the first cycle of loading is considered due to the buildup of excess pore pressures. Hardin & Drnevich's expression is again used for comparison, along with curves fitted to the data of Wilson (1988) who compared material damping in this same sand saturated with 100 cS silicone oil and with water using a resonant column device, at 100 kPa effective confining pressure.

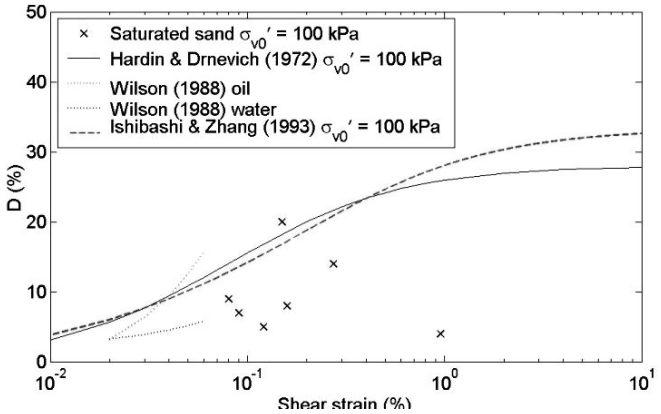

Figure 14. D-γ relationships for saturated sand, σ_{v0}' = 100 kPa

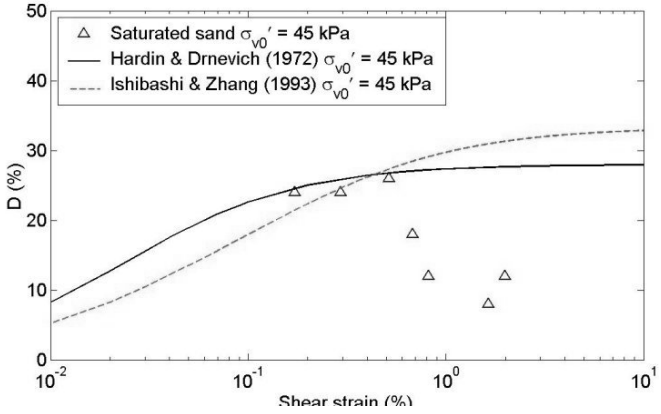

Figure 15. D-γ relationships for saturated sand, σ_{v0}' = 45 kPa

Wilson's data showing increased damping in the presence of a viscous pore fluid had implications for centrifuge modellers, who are often constrained to use such a fluid for

the correct modelling of seepage velocities (e.g. Schofield, 1980). But in Figure 14, the 100 kPa data points around 0.1 % strain appear to fall more towards an extrapolation of his water-saturated models than the oil-saturated tests. The mechanism of pore fluid viscosity increasing damping at 1-g could therefore be related to rate of fluid movement through voids. This process is accelerated during centrifuge testing, which is why viscous pore fluid is used in the first place. It would appear as if material damping in centrifuge models should match the prototype providing the correct viscosity is used for the appropriate g-level.

The second interesting point from these plots is the behaviour at strains above0.6%. These data points, which have all come from stress-strain loops deemed to be representative of hysteretic damping, show a marked drop in calculated damping ratio where the value should plateau at a D_{max}. What is probably happening is that by applying such large strains the soil has immediately been taken into a state approaching complete liquefaction. With the soil now operating in a different behaviour regime, it appears as if the damping of liquefied soil is much reduced. What are the possible sources for material damping in saturated sand? Frictional energy loss in the soil skeleton is now significantly reduced as the soil particles lose contact with each other. If the pore fluid has hysteretic damping, this should remain constant, depending on how it responds to the associated pressure increase. It would not be expected that this contributes much to the overall damping ratio (Wilson, 1988). Fluid-movement induced energy loss as discussed in section 5.2 will be very much reduced because consolidation coefficient (ratio of permeability to compressibility times unit weight) increases threefold as excess pore pressure ratio increases from about 0.6 to 0.95, and goes up to an apparent value approaching 1000 in liquefied conditions (Brennan, 2004).

Obviously the data here is limited in quantity, but it is intriguing that the first-cycle strain required to cause damping to deviate from the expected curves, here around 0.6%, appears more like a cut-off rather than a gradual effect.

5.3 Normally Consolidated Clay

E-grade kaolin clay as described in section 4.3 was used to derive the damping data in Figure 16, along with damping data from the sources used to compare shear modulus above.

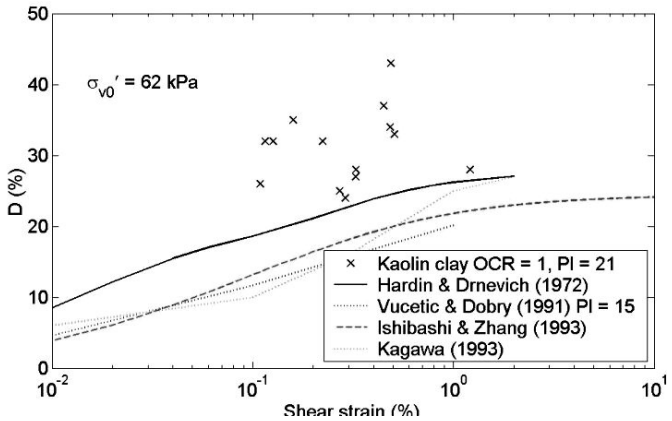

Figure 16. D-γ relationships for N-C clay, PI = 21, σ_{v0}' = 62 kPa

Data collected since the original Hardin & Drnevich work make this equation look like an overprediction, but surprisingly the centrifuge data suggests that the damping obtained during the centrifuge experiment is about 1.5 times the established curves for such material. It would be expected that damping reach an asymptotic value D_{max} at large strains, which is equal to about 28% in Hardin & Drnevich, but rarely do laboratory tests employ sufficiently high strains to achieve such a plateau. And large damping values (up to 45%) have been recorded, by Techavorainskun et al (2001) in cyclic loading tests inducing strains around 10% for example.

It is widely acknowledged that strain rate has an effect on damping in clayey soils, but this has rarely been quantified. Such a relationship would have implications for dynamic centrifuge testing of soft clay, where applied shaking frequencies are necessarily tens of times larger than the prototype frequency interpreted. Here, frequencies around 50 Hz are interpreted as being 1 Hz. The only real difference between the centrifuge experiment and the laboratory tests is the shaking frequency. Based on this evidence, it is suggested that dynamic material damping in clays increases by 1.5 times when frequency is increased from 1 Hz to 50 Hz, and as such caution must be exercised when analysing the results of dynamic centrifuge tests on clayey soils. The effect of this increased hysteretic damping would be a reduction in soil natural frequency and in the response amplitude of surface structures.

5.4 Model Municipal Solid Waste

Model MSW as described in section 4.4 was used to determine whether the damping of this material is representative of real waste. Figure 17 shows the calculated damping from centrifuge data along with bounds from Matasovic & Kavazanjian (1998) and Augello et al (1998) as above.

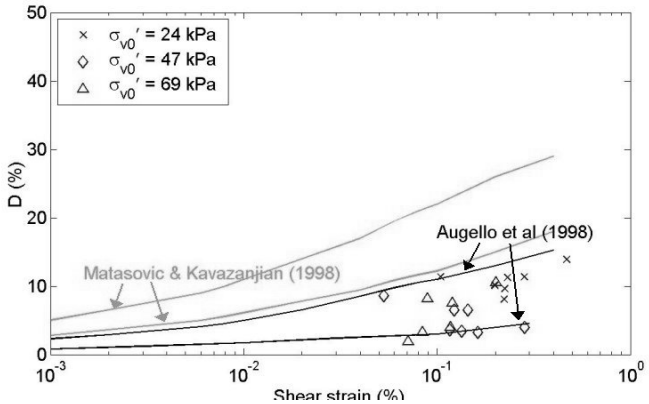

Figure 17. D-γ relationships for model MSW

The published bounds surprisingly show mutually exclusive areas, indicating the variability in both landfill material (even from the same site) and in the equivalent damping ratio as a parameter. Centrifuge data provides a good match with the Augello bounds, indicating that the value is representative of a real MSW.

As with previous values from this study, a large degree of scatter is seen. It would appear as if damping ratio as a parameter cannot be determined any more (or less) accurately by centrifuge testing than alternative methods. Given the wide variability in possible values for this parameter, both in the current study and previous research, it would be advisable that analyses carried out are not strongly influenced by small changes in the input value of damping. This would apply to all soils within the range tested in this paper.

6 Discussion

Shear modulus values obtained from all centrifuge tests appear to be relatively close to the relevant published degradation curves, with a degree of scatter comparable to that observed in many other investigations. This required the parameter G_{max} to be obtained from the actual test, as analyses using the Hardin & Drnevich (1972b) equation for small strain stiffness found it to overestimate the soil stiffness. Shear wave velocities obtained

from depth averages between datapoints make a surprising source of good G_{max} information as even the "small strain" air hammer imparts strains around 0.03%. Being a more reliable parameter than damping, it is perhaps not surprising that existing approximations for G-γ curves proved to be suitable for all materials tested here.

The values of damping achieved were subject to more scatter, as might be expected from integrating non-elliptical shape of the traces. It is necessary, though, not to convert figures to equivalent ellipses as discussed in section 3.4. The dry sand and the model waste behaved in accordance with the data of other researchers indicating that these materials do not undergo significant parameter changes during centrifuge testing. Saturated sand also behaved as expected, prior to excess pore pressure build up. Testing on saturated samples would ordinarily be performed without the potential for excess pore pressure generation (dense soils or drained conditions, e.g.) so this case should match. Post-liquefaction damping behaviour has not been investigated by other researchers, and the noticeable reduction measured in these tests has implications for computer codes dealing with such parameters. Further work could quantify the altered damping degradation curves for liquefying sands. Clay did not share damping in common with expected results. This was explained above in terms of the applied shaking frequency. Earthquake and laboratory test loading frequencies are of the same order of magnitude, around 1 Hz, whereas centrifuge tests at N times earth's gravity require vibrations to be N times faster. Dynamic centrifuge testing on clayey materials should be interpreted with caution as an excessively large damping ratio could operate. Sands appeared to be unaffected by such frequency effects, in this work.

7 Conclusions

Centrifuge accelerometer data has been used to produce shear stress-strain loops. Several important considerations have been described to ensure high quality results are obtained. This particularly applies to back-calculation of damping ratios, which have been shown to occasionally suffer from an interesting effect where small anticlockwise loops may be present. These have a negative contribution to calculated damping and if their presence is significant then influences other than material damping are in action. Damping ratios should not be calculated based on equivalent ellipses if multiple loading frequencies are being dealt with.

Shear modulus values obtained for all materials examined were appropriate when a suitable value for small strain modulus G_{max} was used. The value of G_{max} obtained from the Hardin & Drnevich (1972b) expression was universally too stiff to enable an accurate data fit. Such a value is only required for producing degradation curves anyway, in which case it is recommended to obtain G_{max} directly from test data if possible.

Equivalent damping ratios obtained were mostly as expected. Judging by the scatter, values obtained were comparable in accuracy and repeatability to alternative methods in use. It would be recommended that analyses utilising these values not be heavily dependent on a precise damping value. The exceptions were saturated sand, and clay. In saturated sand, excess pore pressure generation at strains above 0.6% caused a sharp reduction in damping compared to the expected values. Back-calculated damping ratios for clays were much higher than expected, by a factor of about 1.5. This is attributed to the higher frequency loading applied on the centrifuge.

Acknowledgements

Centrifuge tests were carried out with the excellent assistance of technical staff at the Schofield Centre, Cambridge, which is acknowledged with thanks.

Appendix I. References

1. Abdel-Ghaffar, A.M. & Scott, R.F. (1979) "Shear moduli and damping factors of earth dam". Journal of the Geotechnical Engineering Division, ASCE. 105(12): 1405-1426.
2. Arulnathan, R., Boulanger, R.W., Kutter, B.L. & Sluis, W.K. (2000) "New Tool for Shear Wave Velocity Measurements in Model Tests". Geotechnical Testing Journal. **23**(4) p. 444-453.
3. Augello, A.J., Bray, J.D., Abrahamson, N.A. & Seed, R.B. (1998) "Dynamic properties of solid waste based on back-analysis of OII landfill". Journal of Geotechnical and Geoenvironmental Engineering, ASCE. 124(3): 211-222.
4. Brennan, A.J. (2004) "Vertical drains as a countermeasure to earthquake-induced soil liquefaction". PhD thesis, University of Cambridge, UK.

5. Brennan, A.J., Madabhushi, S.P.G. & Bolton, M.D. (2002) "Behaviour of a suction caisson in soft clay, under monotonic and earthquake loading". Cambridge University Technical Services report to KW Consultants Ltd.
6. Chang, C.-Y., Power, M.S., Tang, Y.K. & Mok, C.M. (1989) "Evidence of nonlinear soil response during a moderate earthquake". Proc. 12th ICSMFE, Rio de Janeiro, Brazil. A.A. Balkema publishers. p. 1927-1930.
7. Ellis, E.A., Soga, K., Bransby, M.F. & Sata, M. (1998) "Effect of pore fluid viscosity on the cyclic behaviour of sands". Proc. Centrifuge 98 (ed. T. Kimura, O. Kusakabe & J. Takemura), Tokyo, Japan. A.A. Balkema publishers. p. 217-222.
8. Ghosh, B. & Madabhushi, S.P.G. (2002) "An efficient tool for measuring shear wave velocity in the centrifuge". Proc. Int. Conf. on Physical Modelling in Geotechnics (ed. R. Phillips, P.J. Guo & R. Popescu), St Johns, NF, Canada. A.A. Balkema publishers. p. 119-124
9. Hardcastle, J.H. & Sharma, S. (1998) "Shear modulus and damping of unsaturated loess". Geotechnical Earthquake Engineering and Soil Dynamics III, ASCE Geotechnical Special Publication 75 p. 178-188.
10. Hardin, B.O. & Drnevich, V.P. (1972a) "Shear modulus and damping in soils: Measurement and parameter effects". Journal of Soil Mechanics and Foundations Division, ASCE. 98(6): 603-624.
11. Hardin, B.O. & Drnevich, V.P. (1972b) "Shear modulus and damping in soils: Design equations and curves". Journal of Soil Mechanics and Foundations Division, ASCE. 98(7): 667-692.
12. Idriss, I.M., Dobry, R. & Singh, R.D. (1978) "Nonlinear behavior of soft clays during cyclic loading". Journal of the Geotechnical Engineering Division, ASCE. 104(12): 1427-1447.
13. Ishibashi, I. & Zhang, X. (1993) "Unified dynamic shear moduli and damping ratios of sand and clay". Soils and Foundations 33(1): 182-191.
14. Kagawa, T. (1993) "Moduli and damping factors of soft marine clays". Journal of Geotechnical Engineering, ASCE. 118(9): 1360-1375.
15. Kokusho, T. (1980) "Cyclic triaxial test of dynamic soil properties for wide strain range". Soils and Foundations 20(2): 45-60.
16. Kokusho, T., Yoshida, Y. & Esashi, Y. (1982) "Dynamic properties of soft clay for wide strain range". Soils and Foundations 22(4): 1-18.

17. LoPresti, D.C.F., Jamiolkowski, M., Pallara, O., Cavallaro, A. & Pedroni, S. (1997) "Shear modulus and damping of soils". Géotechnique 47(3): 603-617.
18. Madabhushi, S.P.G., Schofield, A.N. & Lesley, S. (1998) "A new stored angular momentum (SAM) based actuator". Proc. Centrifuge 98 (ed. T. Kimura, O. Kusakabe & J. Takemura), Tokyo, Japan. A.A. Balkema publishers. p. 111-116.
19. Matasovic, N. & Kavazanjian, E. (1998) "Cyclic characterization of OII landfill solid waste". Journal of Geotechnical and Geoenvironmental Engineering, ASCE. 124(3): 197-210.
20. Pitilakis, K., Kirtas, E., Sextos, A., Bolton, M.D., Madabhushi, S.P.G. & Brennan, A.J. (2004) "Validation by centrifuge testing of numerical simulations for soil-foundation-structure systems". Proc. 13th World Conf. on Earthquake Engineering, Vancouver, B.C., Canada. Paper no. 2772.
21. Rollins, K.M., Evans, M.D., Diehl, N.B. & Daily, W.D. (1998) "Shear modulus and damping relationships for gravels". Journal of Geotechnical and Geoenvironmental Engineering, ASCE. 124(5): 396-405.
22. Schofield, A.N. (1980) "Cambridge geotechnical centrifuge operations". Géotechnique 30(3): 227-268.
23. Seed, H.B., Wong, R.T., Idriss, I.M. & Tokimatsu, K. (1986) "Moduli and damping factors for dynamic analyses of cohesionless soils". Journal of Geotechnical Engineering, ASCE. 112(11): 1016-1032.
24. Teachavorasinskun, S., Thongchim, P. & Lukkunaprasit, P. (2001) "Shear modulus and damping ratio of a clay during undrained cyclic loading". Géotechnique 51(5): 467-470.
25. Teymur, B. & Madabhushi, S.P.G. (2002) "Shear stress-strain analysis of sand in ESB model container by harmonic wavelet techniques". Proc. Int. Conf. on Physical Modelling in Geotechnics (ed. R. Phillips, P.J. Guo & R. Popescu), St Johns, NF, Canada. A.A. Balkema publishers. p. 201-206.
26. Thusyanthan, I., Madabhushi, S.P.G. & Singh, S. (2004a) "Modelling the seismic behaviour of municipal solid waste". Proc. 11th Int. Conf. on Soil Dynamics & Earthquake Engineering/3rd Int. Conf. on Earthquake Geotechnical Engineering (ed. D. Doolin, A. Kammerer, T. Nogami, R.B. Seed & I. Towhata). University of California, Berkeley, CA, USA. Vol. 2, p. 283-290.

27. Thusyanthan, I., Madabhushi, S.P.G., Singh, S., Haigh, S.K. & Brennan, A.J. (2004b), "Seismic Behaviour of Municipal Solid Waste Landfills", Proc. 13th World Conference on Earthquake Engineering, Vancouver, B.C., August 2004.
28. Vucetic, M. & Dobry, R. (1991) "Effect of soil plasticity on cyclic response". Journal of Geotechnical Engineering, ASCE.117(1): 89-107.
29. Wilson, J.M.R. (1988) "A theoretical and experimental investigation into the dynamic behaviour of soils". PhD thesis, University of Cambridge, UK.
30. Zeghal, M. & Elgamel, A.W. (1994) "Analysis of site liquefaction using earthquake records". Journal of Geotechnical Engineering, ASCE. 120(6): 996-1017.
31. Zeghal, M., Elgamel, A.W., Tang, H.T. & Stepp, J.C. (1995). "Lotung Downhole Array. II: evaluation of soil nonlinear properties". Journal of Geotechnical Engineering, ASCE. 121(4): 363-378.

Appendix II. Notation

The following symbols are used in this paper:-

D = Equivalent damping ratio

D_{50} = Sieve size with 50% by mass passing

e_{min}, e_{max} = Minimum and maximum void ratios

f_0 = Fundamental natural frequency

G = Secant shear modulus

G_{max} = Maximum (small-strain) shear modulus

H = Soil layer thickness

u, $\ddot{u}$ = Horizontal displacement/acceleration

V_s = Shear wave velocity

W = Total work done

$W_{elastic}$ = Equivalent elastic work done

z = Depth below soil surface

γ = Strain

σ_{v0}' = Initial vertical effective stress

ρ = Bulk density

τ = Shear stress

Appendix III. MatLab® Codes

The following codes are those written especially for the purpose based on MatLab release 12 in mid-2004. Function StressStrainWizard is the controlling entity, a graphical-user-interface with which the user may load files and choose instruments to interpret. The programs require a MatLab data file, containing the following arrays:-

- Data: 1 column per instrument
- coords: 1 column per instrument, row 1 is the x coordinate, row 2 is the y coordinate and row 3 is the z coordinate ie. depth.
- names: A cell array. Each column is a cell containing the instrument name as a string.
- samp: A cell array, containing one cell, which is a string of the data sampling frequency in Hertz.

Outputs: Stress strain loops for selected regions of shaking, shear modulus, damping ratio (if a single cycle is selected).

Operates: Type StressStrainWizard at the MatLab prompt.

GUI Inputs:-

- LOAD: Click here to select the data file. The name will appear in the Filename box automatically once selected. If no file is selected this will just be a zero array and the program won't work. This also puts instrument names in the appropriate boxes.
- Filter Limits: You need a non-zero lower and upper frequency between which to filter. The lower frequency must be on the left! Do not over-filter or under-filter – see above!
- Effective weight: It means, unit weight, in kN/m^3.
- Instrument 1: Topmost instrument in column.
- Instrument 2: Middle instrument in column.
- Instrument 3: Either the deepest instrument of the 3, or if there is insufficient data or a first order estimate only is required, choose the last option "1st order only".
- EXIT: exits the GUI.
- GO: runs the program. This brings up a plot of the calculated stress and strain versus time, which will disappear, and a window of one of the accelerations. Draw a rubber-band box around the region you wish to work out stress and strain loops.

Click "ready" when satisfied to close the stress-time and strain-time plots and proceed to the stress-strain loops.

Additional Information:

If some or all of the instrument name boxes are blank after changing the data file, it is because the names array has gone out of range. Exit the figure, and restart.

StressStrainWizard.m

```
% Use earthquake data to plot shear moduli and damping between pairs
of/groups of three accelerometers.
%
% A.J.Brennan 21/04/2004
%
function StressStrainWizard
%
h0 = figure('Position',[100 300 300 200],...
    'Tag','fig1');

h1 = uicontrol('Parent',h0,...
    'units','pixels',...
    'position',[10 170 80 20],...
    'style','text',...
    'string','Filename :',...
    'tag','text1');
h1 = uicontrol('Parent',h0,...
    'units','pixels',...
    'position',[100 170 190 20],...
    'BackgroundColor',[1 1 1],...
    'style','text',...
    'HorizontalAlignment','right',...
    'string',' ',...
    'tag','filenamebox');
h1 = uicontrol('Parent',h0,...
    'units','pixels',...
    'position',[10 130 80 20],...
    'style','text',...
    'string','Instrument 1:',...
    'tag','text2');
h1 = uicontrol('Parent',h0,...
    'units','pixels',...
    'position',[10 100 80 20],...
    'style','text',...
    'string','Instrument 2:',...
    'tag','text3');
h1 = uicontrol('Parent',h0,...
    'units','pixels',...
    'position',[10 70 80 20],...
    'style','text',...
    'string','Instrument 3:',...
    'tag','text4');

h1 = uicontrol('Parent',h0,...
    'units','pixels',...
    'position',[210 110 80 40],...
```

```
    'style','pushbutton',...
    'string','LOAD',...
    'tag','loadbutton',...
    'Callback', 'ajbgetname3',...
    'BackgroundColor',[1 1 0],...
    'FontSize',12);
h1 = uicontrol('Parent',h0,...
    'units','pixels',...
    'position',[210 60 80 40],...
    'style','pushbutton',...
    'string','GO',...
    'tag','loadbutton',...
    'Callback', '[G,D,gamma] = stressstrainmagic',...
    'BackgroundColor',[0.5 0.8 0.1],...
    'FontSize',12);
h1 = uicontrol('Parent',h0,...
    'units','pixels',...
    'position',[210 10 80 40],...
    'style','pushbutton',...
    'string','EXIT',...
    'tag','loadbutton',...
    'Callback', 'close(gcbf)',...
    'BackgroundColor',[0.9 0.1 0.1],...
    'FontSize',12);
%
h1 = uicontrol('Parent',h0,...
    'units','pixels',...
    'position',[100 130 100 20],...
    'style','popupmenu',...
    'Tag','Instrument1list',...
    'string','waiting...',...
    'value',1);
h1 = uicontrol('Parent',h0,...
    'units','pixels',...
    'position',[100 100 100 20],...
    'style','popupmenu',...
    'Tag','Instrument2list',...
    'string','waiting...',...
    'value',1);
h1 = uicontrol('Parent',h0,...
    'units','pixels',...
    'position',[100 70 100 20],...
    'style','popupmenu',...
    'Tag','Instrument3list',...
    'string','waiting...',...
    'value',1);
%
h1 = uicontrol('Parent',h0,...
    'units','pixels',...
    'position',[10 40 40 20],...
    'style','edit',...
    'Tag','filterlow',...
    'string','15');
h1 = uicontrol('Parent',h0,...
    'units','pixels',...
    'position',[160 40 40 20],...
    'style','edit',...
    'Tag','filterhigh',...
    'string','450');
h1 = uicontrol('Parent',h0,...
    'units','pixels',...
```

```
    'position',[60 40 90 20],...
    'style','text',...
    'Tag','filterlabel',...
    'string','Filter Limits (Hz)');
%
h1 = uicontrol('Parent',h0,...
    'units','pixels',...
    'position',[160 10 40 20],...
    'style','edit',...
    'Tag','densitybox',...
    'string','16');
h1 = uicontrol('Parent',h0,...
    'units','pixels',...
    'position',[10 10 140 20],...
    'style','text',...
    'Tag','gammadashlabel',...
    'string',{'Effective weight (kN/m^3)'});
```

ajbgetname3.m

```
function ajbgetname3
[f,p] = uigetfile('*.mat','Load processed CDAQS workspace');
filename = [p,f];
Hnd1 = findobj(gcbf,'Tag','filenamebox');
set(Hnd1,'String',filename);
%
load(filename, 'names')
Hnd2 = findobj(gcbf,'Tag','Instrument1list');
set(Hnd2,'string',names);
Hnd3 = findobj(gcbf,'Tag','Instrument2list');
set(Hnd3,'string',names);
Hnd4 = findobj(gcbf,'Tag','Instrument3list');
composite = {names{:},'1st order only'};
set(Hnd4,'string',composite);
```

stressstrainmagic.m

```
% Stressstrainmagic is called by the GO button of StressStrainWizard.
% Calculates stress-strain loops and damping ratios, based on a
% second order interpolation between three accelerometers in a
vertical
% plane. Needs a CDAQS data file.
%
% A.J.Brennan 27/04/2004
%
function [G,D,gamma] = stressstrainmagic
global sut
%
% Locate all the variables required from the call back figure
h1 = findobj(gcbf,'Tag','Instrument1list');
h2 = findobj(gcbf,'Tag','Instrument2list');
h3 = findobj(gcbf,'Tag','Instrument3list');
h4 = findobj(gcbf,'Tag','filenamebox');
h5 = findobj(gcbf,'Tag','densitybox');
%
instrument1 = get(h1,'value');
instrument2 = get(h2,'value');
instrument3 = get(h3,'value');
filename = get(h4,'string');
fname = filename(length(filename)-12:length(filename));
```

```
density = 1000*str2num(get(h5,'string'))/10; % Density in kg/m^3
%
load(filename); % Loads CDAQS data file, containing Data, names,
coords, samp
fs = str2num(samp{1});
time = [0:size(Data,1)-1]/fs;
%
% Evaluate whether 1st or 2nd order approximation is to be used.
% 1st order is achieved by selecting the relevant option in the
% instrument 3 listbox.
if instrument3 > length(names),
    order = 1;
else
    order = 2;
end
%
% Retrieve filter characteristics from GUI.
h1 = findobj(gcbf,'Tag','filterlow');
h2 = findobj(gcbf,'Tag','filterhigh');
Wn = [str2num(get(h1,'string')), str2num(get(h2,'string'))]*2/(fs);
b = fir1(512,Wn);
%
% Now we need to cut off the parts of the signal that are not due to
% applied shaking.
debut = 1; fin = length(Data(:,1));
while abs(Data(debut,instrument1)) < 0.3,
    debut = debut + 1;
end
while abs(Data(fin,instrument1)) < 0.4,
    fin = fin - 1;
end
Data2(1:debut-1,:) = zeros(debut - 1, size(Data,2));
Data2(debut:fin,:) = Data(debut:fin, :);
Data2(fin+1:size(Data,1),:) = zeros(size(Data,1)-fin, size(Data,2));
%
switch order
case 1
    % First order approximation requires only two instruments.
    % We can now define our accelerometer array, and filter same.
    accs = filtfilt(b,1,Data2(:, [instrument1; instrument2]));
    depth = [coords(3,instrument1); coords(3,instrument2)];
    titlab = ['Instruments ', names{instrument1}, ' and ',
names{instrument2}];
case 2
    % Second order approximation requires three instruments.
    % We can now define our accelerometer array, and filter same.
    accs = filtfilt(b,1,Data2(:, [instrument1; instrument2;
instrument3]));
    depth = [coords(3,instrument1); coords(3,instrument2);
coords(3,instrument3)];
    titlab = ['Instruments ', names{instrument1}, ',
',names{instrument2}, ' and ', names{instrument3}];
    %
end
%
% Check if depths are measured from the base of the box.
% In this case, they are really heights and must be subtracted from
total layer
% thickness to be useable in the equations.
if depth(1) > depth(2),
```

```
    thickness = inputdlg('Enter depth of soil (mm)','Crazy stress-
strain action',1,{'340'});
    depth = str2num(thickness{1}) - depth;
end
%
accs = 10*accs;    % In metres/s^2;
depth = depth/1000; % In metres;
%
% Apply integration to the accelerations to obtain velocity.
% This must be filtered before reintegrating.
vels = filtfilt(b,1,cumtrapz(time,accs));
disp = cumtrapz(time,vels);
%
% Now we can get back to the calculation of stress and strain.
% The equations SHOULD BE CHECKED prior to use; know whether they
work
% for your application.
%
shearstrain = calculatestrain(depth, disp);
shearstress = calculatestress(depth, accs, density);
%
% Select limits between which to draw loops/calculate damping.
[point1, point2] = picklimits(accs(:,1),fs);
%
stress = shearstress(point1:point2)/1000;   %In kPa
strain = 100*shearstrain(point1:point2) ;      %In percent
%
G = 0.1*(max(stress) - min(stress))/(max(strain) - min(strain)); %In
MPa

% Now to calculate damping...
%
Area = cumtrapz(strain, stress);
Elasticarea = 0.25*(max(stress)-min(stress))*(max(strain)-
min(strain));
%
D = 100*Area(length(Area))/(2*pi*Elasticarea); %In percent
%
% Here's the plotting section
if ishandle(5) == 1,
    close(5);
end
figure(5)
hold on
%fill(strain,stress,'c')
hline1 = plot(strain,stress,'b-')
hline2 = plot([min(strain), max(strain)],[min(stress),
max(stress)],'r--')
%xlimits = max([max(strain);abs(min(strain))]);
%ylimits = max([max(stress);abs(min(stress))]);
%set(gca,'XLim',[-xlimits; xlimits], 'YLim',[-ylimits; ylimits]);
set(gca,'FontSize',14);
set(hline2, 'LineWidth', 2)
xlabel('Shear Strain \gamma (%)'); ylabel('Shear Stress \tau (kPa)');
addedtext{1} = ['G = ', num2str(round(G)), ' MPa'];
addedtext{2} = ['D = ', num2str(round(D)), '%'];
addedtext{3} = ['Time = ', num2str(time(point1)),' s to
',num2str(time(point2)),' s'];
h1 = text(0, 0.8*min(stress), addedtext);
%h2 = text(min(strain),0.9*max(stress), {fname});
set(h1,'fontsize',14,...
```

```
    'FontWeight','bold');
set(5,'Position',[420 225 560 420])
title(titlab)
grid on; hold off
%
if ishandle(11) == 1,
    close(11);
end
gamma = 0.5*(max(strain) - min(strain));
residual = 100*(max(strain) - gamma)/max(strain)
```

calculatestrain.m

```
% Two ways of obtaining shear strain:
% First, simple interpolation, relative displacement over separation
distance.
% Second, copied from Zeghal & Elgamel's paper.
%
function [g] = calculatestrain(z, u)
order = size(u,2) - 1;
switch order
case 1
    g = (u(:,2) - u(:,1))/(z(2) - z(1));
case 2
    dz = [z(2) - z(1), z(3) - z(2), z(3) - z(1)];
    g = (((u(:,3) - u(:,2))*dz(1)/dz(2)) +...
        ((u(:,2) - u(:,1))*dz(2)/dz(1)))/dz(3);
end
peakstrains = [max(g); min(g)];
figure(11)
subplot(2,1,2)
plot(g*100,'r'); ylabel('Shear strain (%)')
```

calculatestress.m

```
% Based on,
% T(z) = 0.5*rho*z*(surface acceleration + acceleration at depth z)
% Zeghal & Elgamel quote this.
%
function [T] = calculatestress(z,a,density)
%
asurf = a(:,1) + z(1)*(a(:,1)-a(:,2))/(z(2)-z(1));
T = 0.5*density*z(2)*(asurf + a(:,2));
%
% This line is interchangeable but more cumbersome.
% T = 0.5*density*(a(:,1)*z(2)*z(2) - 2*a(:,2)*z(1)*z(2) +
a(:,2)*z(2)*z(2))/(z(2)-z(1));
%
peakstresses = [max(T); min(T)];
figure(11)
subplot(2,1,1)
plot(T/1000); ylabel('Shear stress (kPa)')
```

picklimits.m

```
% A function for choosing the limits based on a graphical plot of
% an acceleration (or other) trace. No time base required, just
% sample space.
%
```

```
% 27/04/04 A.J.Brennan
%
function [dechrau, diwedd] = picklimits(acc,fs)
global sut
%
figure(19)
set(19,'units','pixels',...
    'position',[100 150 500 400],...
    'menubar','figure');
zoom
%
h1 = plot([0:length(acc)-1]/fs,acc);
title('Select region for analysis');
h2 = gca;
set(h2,'units','pixels',...
    'position',[45 100 410 270],...
    'Tag','squiggle');

h3 = uicontrol('style','pushbutton',...
    'string','Ready',...
    'units','pixels',...
    'position',[200 10 100 40],...
    'fontsize',12,...
    'BackGroundColor',[0.4 0.8 0.2],...
    'callback','sut = getthoselimits;');
uiwait(19)
%
% dechrau and diwedd respectively mean start and end, in Welsh.
%
dechrau = round(fs*sut(1));
diwedd = round(fs*sut(2));
```

getthoselimits.m

```
function [sut] = getthoselimits(hndl)
global sut
if nargin < 1,
    hndl = findobj(19,'Tag','squiggle');
end
sut = get(hndl,'XLim');
close(gcbf)
```